Journal of Nuclear Materials 568 (2022) 153897

Contents lists available at ScienceDirect

Journal of Nuclear Materials

journal homepage: www.elsevier.com/locate/jnucmat

Deuterium retention and desorption behavior of W-Ta-Cr-V high entropy alloy

Yongzhi Shi[a], Zhenyu Jiang[a], Tongjun Xia[a], Zizhao Wang[a], Jianwei Wu[a], Xingzhong Cao[c], Kaigui Zhu[a,b,*]

[a] Department of Physics, Beihang University, Beijing 100191, China
[b] Beijing Key Laboratory of Advanced Nuclear Energy Materials and Physics, Beihang University, Beijing 100191, China
[c] Institute of High Energy Physics, Chinese Academy of Sciences, Beijing 100049, China

ARTICLE INFO

Article history:
Received 13 April 2022
Revised 6 June 2022
Accepted 28 June 2022
Available online 30 June 2022

Keywords:
Tungsten films
High-entropy alloy films
Magnetron Sputtering
Deuterium plasma irradiation
Deuterium retention

ABSTRACT

Deuterium retention and desorption behavior of W-Ta-Cr-V films under deuterium plasma irradiation were studied. The W-Ta-Cr-V films were prepared on the molybdenum (Mo) substrate by magnetron sputtering. Subsequently, all films annealed at 1000 °C were exposed to deuterium plasma at a flux of 8.13 × 10^{19} D/m^2·s for 9 h to achieve an irradiation fluence of 2.63 × 10^{24} D/m^2. Electron backscattered diffraction (EBSD) was used to characterize the texture and average grain size of films. Doppler broadening spectrometry of positron annihilation (DBS-PA) was carried out with an energy-variable slow positron beam to detect the concentration of vacancy-type defects in the films. The results suggest that there are fewer vacancy-type defects inside W-Ta-Cr-V grains. Deuterium retention and the desorption behavior of W-Ta-Cr-V were studied by compared to pure tungsten films. In the 300–800 K temperature range, the peaks of thermal desorption spectroscopy (TDS) of W-Ta-Cr-V films are substantially consistent with that of the W films. Notably, in the range of 800 K-1000 K, W-Ta-Cr-V film has no thermal desorption peak. We attribute this to the large lattice distortion and low vacancy formation energy, which inhibit the growth of voids inside the grains of W-Ta-Cr-V films. The total deuterium retention of W-Ta-Cr-V films is compared with that of W films. It is measured by TDS that the deuterium retention of W-Ta-Cr-V films is nearly 5 times that of W films. Based on the analysis of the TDS spectra, the higher deuterium retention in W-Ta-Cr-V films is due to the more grain boundary defects.

1. Introduction

Currently, high entropy alloys (HEAs) [1,2], as a new solid solution alloy material, have become one of the prominent candidate materials used in advanced nuclear energy system reactors due to their excellent high-temperature comprehensive performance (e.g., high-temperature stability, high-temperature strength, and radiation resistance, etc.). The exceptional performance of HEAs is generally understood in terms of high entropy effect [3], severe lattice-distortion effect [4] and sluggish diffusion effect [5]. Among them, the high configuration entropy reduces the Gibbs free energies of the HEA system, which makes the system tend to form a stable solid solution structure. And, the excellent high-temperature strength and high-temperature stability of HEAs originate from their unique inherent characteristics of severe lattice distortion and sluggish diffusion due to the atomic size mismatch difference among different elements [6]. Nowadays, the plasma-facing materials (PFMs) in the magnetic confinement fusion device (Tokamak) are required to have good radiation resistance, because they face high thermal load and bombardment by strong particle flux during service. For the PFMs of Tokamak, the PFMs must be able to simultaneously withstand three conditions, including 14.1 MeV fusion neutron, high thermal load and high flux plasma (10^{24} $m^{-2}s^{-1}$) of hydrogen isotopes (D and T), helium (He). It is well known that the generation and aggregation evolution of defects under high-energy irradiation are the fundamental reasons which caused the material performance degradation [7,8]. The complexity of the multi-principal components of HEAs changes the intrinsic properties of the materials and affects the generation of point defects and the short-range recombination process. Studies have shown that the defect evolution process in HEAs under high-energy heavy particle irradiation is retarded through tuning the energy dissipation and the defect formation and migration energies [9–12].

So far, studies on the radiation of HEAs have been mainly focused on high-energy helium ion and heavy-ion irradiation and there has been little work on the plasma irradiation of HEAs. Xia

* Corresponding author.
E-mail address: kgzhu@buaa.edu.cn (K. Zhu).

https://doi.org/10.1016/j.jnucmat.2022.153897
0022-3115/

et al. [13] found that the Al_xCoCrFeNi (x=0.1, 0.75 and 1.5) HEAs under Au-ions showed exceptional structural stability when irradiated up to over 50 dpa at 298 K, and the irradiation-induced volume swellings in Al_xCoCrFeNi HEAs were significantly lower than conventional nuclear materials. Furthermore, the He-ion irradiation resistance of HEA CrMnFeCoNi by comparison study with a pure Ni and a 304 stainless steel (304SS) was investigated by Yang et al. [14]; they found that the HEA CrMnFeCoNi possesses the smallest He bubble size, the densest SFs/SFTs, and the highest hardening, indicating the best structural stability, as well as the best He-ion irradiation resistance. Therefore, HEAs expands the design space of irradiation-resistant materials and provides a new choice for PFMs of fusion reactors.

Recently, a quaternary W-Ta-Cr-V high-entropy alloy film with a body-centered cubic (*bcc*) single-phase structure has been reported, which has attracted extensive attention [15]. It is worth noting that in this reference there was no radiation-induced dislocation-loop discovered under 1 MeV heavy ion (Kr^{+2}) irradiation at 1073 K at a dose rate of 1.6×10^{-3} dpa·s^{-1} and a dose level of 8 dpa. Moreover, the defect energetics of W-Ta-Cr-V high-entropy alloy using *ab* initio simulation have found that the more severe lattice distortion compared to previous HEAs with face-centered cubic (*fcc*) structure [16]. Because of the large lattice distortion, interstitials in HEAs can only be formed at some particular locations, which helps to understand the irradiation performance of these novel body-centered cubic (bcc) HEAs. More importantly, the improvement of the defect recombination rate is manifested by a large overlap between the migration energies of vacancies and interstitials, which effectively improves the radiation resistance performance of materials. Given this, the deuterium plasma irradiation effect of W-Ta-Cr-V high-entropy alloy needs further research. In this work, W-Ta-Cr-V films were prepared by a magnetron sputtering deposition, we focused our attention on the deuterium retention and desorption behavior of the HEA material under deuterium plasma irradiation.

2. Experiments

2.1. Sample preparation

The sputtering target selects high-purity metal powders of tungsten, tantalum, chromium, and vanadium as raw materials, and weigh them according to the atomic ratio of 38:36:15:11. Subsequently, the alloy powder is loaded into a V-shaped mixer and thoroughly mixed. A circular quaternary alloy composition target material pressed by the hot isostatic pressing method with a diameter, thickness and purity are 60 mm, 4 mm and 99.95%, respectively. All films were deposited with the power of 100 W in direct current (DC) mode using a magnetron sputtering system on molybdenum (Mo) substrates. Powder metallurgy sintered commercial Mo and W materials (with a purity of 99.95%) were purchased from Advanced Technology & Materials Co., Ltd (AT&M; Beijing, China). The Mo substrates with a size of 10 mm × 10 mm × 1 mm were polished to a mirror surface with a polishing machine. Then, ultrasonically cleaned in acetone, ethanol sequentially for 15 min and dried using compressed air after each cleaning cycle. A sample holder with a heater is mounted at a distance of 6 cm directly above the target. The deposition system was evacuated to a background pressure lower than 5×10^{-4} Pa, and then pure Ar gas (99.99%) with a flow rate of 10 standard-state cubic centimeters per minute (sccm) providing the deposition pressure of 0.5 Pa [17]. Similarly, the W films are deposited on the molybdenum (Mo) substrate under the same experimental parameters as described above. The thicknesses of W film and W-Ta-Cr-V film were ~7 μm with a deposition time of 4 h. All samples were annealed at 1000 °C for 1 hour.

2.2. Irradiation experiment

The irradiation experiment was carried out on Beihang-ICP equipped with an ICP source. The chamber was evacuated down to 5×10^{-4} Pa before the operation of irradiation. High-purity D_2 (purity: 99.99%) gas at a flow rate of 30 sccm enters the plasma source through the top of the equipment. High-density uniform plasma is generated by radio-frequency (RF) discharge produced using inductive coupling of 13.56 MHz RF to a 6-loop spiral coil surrounding a quartz tube with a diameter of 10 cm [18]. The RF power and working pressure in the quartz tube were fixed at 300 W and 0.25 Pa. During the deuterium plasma irradiation, the plasma energy was 110 eV and the film temperature reached a steady level of 573 K detected by thermocouple. The total irradiation fluence was 2.63×10^{24} D/m^2 achieved with an average flux intensity of 8.13×10^{19} D/m^2·s for 9 h.

2.3. Analysis

Grazing incidence X-ray diffraction (GIXRD) was employed for the determination of the crystal structure phases of films. A scanning electron microscope (SEM) was used to observe the fracture surface morphologies of films. The element composition ratio of W-Ta-Cr-V films was characterized by Energy-dispersive x-ray spectroscopy (EDS). The EBSD instrument equipped with a field emission gun (FEG-SEM) was employed to examine the texture and grain size information of the films. Nano indenter G200 in Tsinghua University with a Berkovich indenter was employed to measure the hardness of the films with a continuous stiffness measurement (CSM) technique. Each sample was tested ten points and the results were the average of ten values. Since the elastic stress fields beneath the indenter are sensitive to microstructure features that are up to ~10 times the indenter depth, the maximum extent of the near-surface ion irradiated region that was unaffected by the underlying (softer) unirradiated substrate was kept at ~10% of the film thickness.

Doppler broadening spectrometry of positron annihilation (DBS-PA) test has high sensitivity to characterize vacancy-type defects [19]. The variable energy slow positron beam was carried out at room temperature in the Key Laboratory of Nuclear Analysis Technology, Institute of High Energy Physics (IHEP), Chinese Academy of Sciences. The diameter of the slow positron beam is 8 mm, and the energy range is 0.18~20.18 keV. In this work, slow positrons were utilized to obtain information on the difference in vacancy-type defect concentration between W films and W-Ta-Cr-V films. The high-purity germanium detector recorded gamma rays with an energy of 499.5–522.5 keV during the test. In the measured doppler broadening spectrum, the ratio of the central low-momentum area to the whole spectrum area defines the *S* parameter. Correspondingly, the ratio of the wing high-momentum area to the whole one determines the *W* parameter. The γ ray with an energy range of 510.2–511.8 keV corresponds to the low-momentum zone, and the γ ray with an energy range of 513.6–516.9 keV and 505.1–508.4 keV corresponds to the high-momentum zone. Note that the *S* parameter corresponds to the positron annihilation with the valence electrons, and the *W* parameter corresponds to the positron annihilation with the core electrons. The *S* parameter is sensitive to open volume defects, whereas the *W* parameter is sensitive to the chemical surrounding the annihilation site. The *S* parameter is sensitive to open volume defects and an increase in the *S* parameter indicates an increase in the concentration of vacancy defects in the materials. Considering the very complex reaction between the positrons and the surface, the annihilation data from positrons with energy below 2 keV are not considered here [20].

Subsequently, thermal desorption spectroscopy (TDS) measurement was performed to investigate deuterium desorption behav-

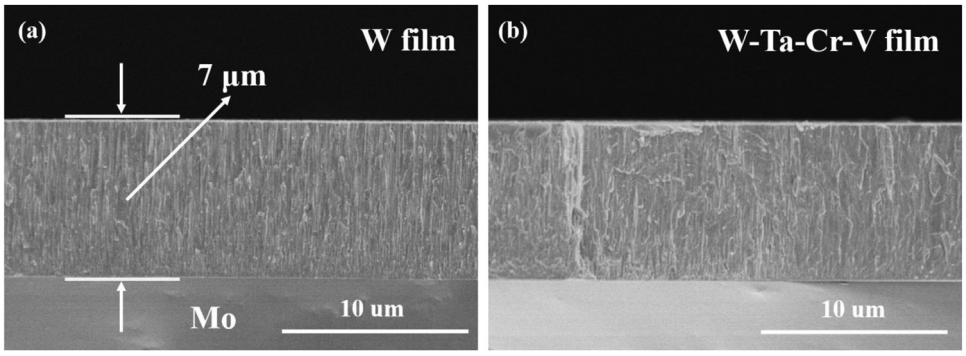

Fig. 1. SEM images of W film and W-Ta-Cr-V film fracture surface.

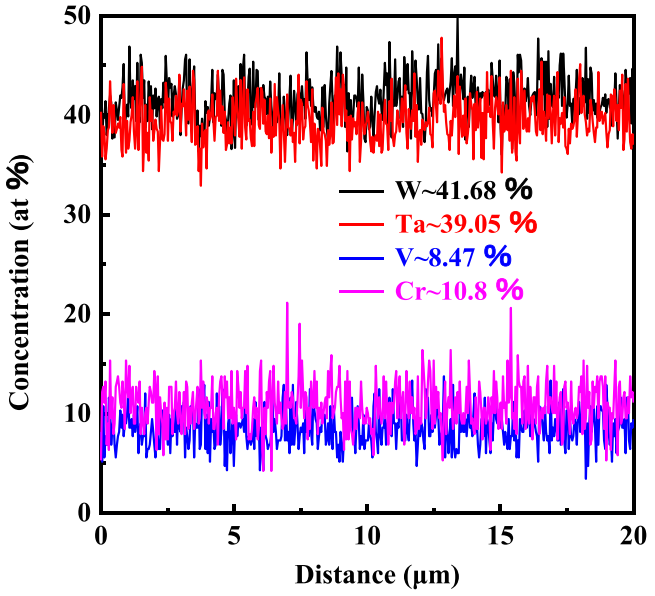

Fig. 2. Alloy composition. EDS line scan concentration profiles of the elements in the W-Ta-Cr-V film.

iors at the temperature range of room temperature (RT) to 1273 K. The time lag between the plasma irradiation and the TDS measurement for each sample was around one month, ensuring that weakly bound and solute deuterium atoms were released during the storage time, so that only the trapped content was observed. Before testing, the background air pressure remained lower than 5×10^{-5} Pa. During the TDS test, the heating rate was maintained at 1 K/s, and a quadrupole mass spectrometer was used to monitor the signals, including HD (mass 3), and D_2 (mass 4).

3. Results

3.1. SEM image of the cross-section of the W film and W-Ta-Cr-V film

A fractured cross-sectional SEM image of the as-deposited W films and W-Ta-Cr-V films is given in Fig. 1. Obviously, films were successfully deposited on Mo substrate and exhibit a fine-grained crystalline microstructure character. The deposition rate was approximately 29.17 nm/min for both films. The thickness of both films was approximately 7 μm at a deposition time of four hours.

3.2. EDS spectrum analysis

The results of EDS test are shown in Fig. 2 to determine the composition of the alloy element in W-Ta-Cr-V films, revealing that

Table 1
The atomic radius (R) and melting temperature (T_m) of the elements in W-Ta-Cr-V films, as well as the δ value (atomic size poly-dispersity) [37].

Elements	W	Ta	Cr	V
Radius (Å)	1.367	1.430	1.249	1.316
T_m (K)	3683	3269	2163	2130
δ	4.126			

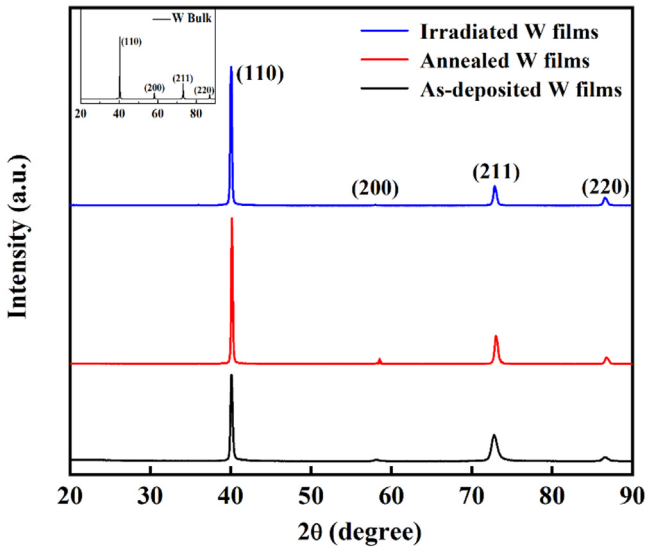

Fig. 3. XRD patterns of the as-deposited, annealed, and irradiated W films.

the four elements of W, Ta, Cr and V are distributed in the films at atomic ratios of 41.68%, 39.05%, 10.8% and 8.47%, respectively, as shown in Table 1. The results of EDS mapping show uniform elemental composition, indicating that there is no significant segregation of the alloy elements in the films.

3.3. X-ray diffraction patterns

The XRD pattern of W films in Fig. 3 shows that the obvious characteristic peaks from the (110), (200), (211), and (220) planes, indicating a typical *bcc* structure W crystalline structure. This is consistent with the crystal structure of W bulk. All tests were performed on the same sample and under the same test conditions. It is shown that the intensity of the diffraction peaks of the annealed W films is significantly enhanced due to the annealing treatment. Optimizing the microstructure of the films through annealing treatment not only reduces defects, but also reduces the residual stress in the films. The diffraction peak intensity of the irradiated W films decreases slightly and the full width at half max-

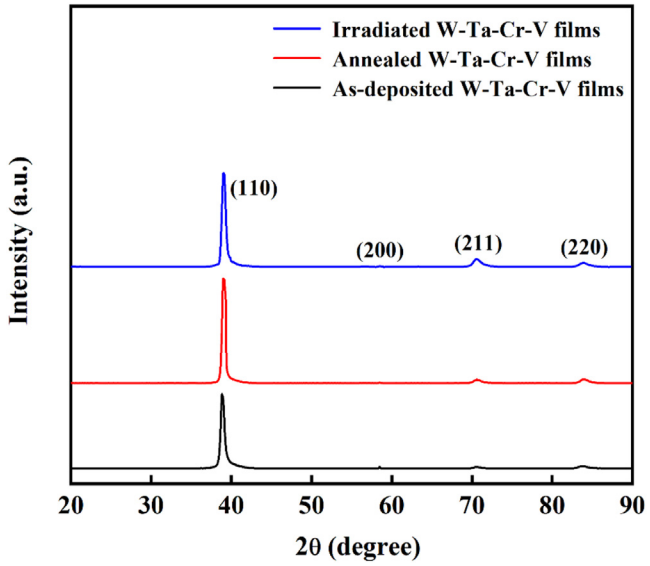

Fig. 4. XRD patterns of the as-deposited, annealed, and irradiated W-Ta-Cr-V films.

ima (FWHM) increases slightly, indicating the defects and microstrains in the lattice structure caused by radiation [21].

The XRD patterns of as-deposited and annealed W-Ta-Cr-V films are presented in Fig. 4. The results show that the *bcc* single-phase solid solution crystal structure is still maintained after annealing at 1000 °C. Compared with pure W films, the films were found to exhibit a larger FWHM and lower peak strength, especially at high angles [22]. We attribute the cause to the intrinsic lattice distortion is expected to result in the significant loss of crystallization perfection and the severe X-ray scattering effect [23]. Therefore, the result is inseparable from the lattice distortion effect in high-entropy alloys.

3.4. EBSD results

EBSD orientation map of W films and W-Ta-Cr-V films used in this study is shown in Fig. 5(a) and (b). Fig. 5(c) shows that the preferred orientations of W-Ta-Cr-V films are (110), which is consistent with the test results of XRD. The average grain sizes of the two films are calculated to be 157.2 nm and 128.3 nm, respectively. At the same time, a bar graph of the grain size statistical distribution is given, as shown in Fig. 6. Ultrafine grains are defined as those having the shortest distance between opposite grain boundaries $<$ 500 nm and nano-crystalline grains as having the shortest distance $<$ 100 nm. Thus, both ultrafine and nanocrystalline grains coexist in the films [24]. In this case, the larger grain size difference can be considered that the W-Ta-Cr-V films have more grain boundary defects than the W films.

3.5. DBS-PA and TDS measurement results

In order to obtain the distribution and characteristic information of vacancy-type defects in W-Ta-Cr-V films, the W films and W-Ta-Cr-V films were sent to IHEP for DBS-PA measurement. Fig. 7 shows the depth distribution of *S* parameters of the two films before deuterium irradiation, from which it can be seen that *S* parameters are approximately consistent within the detection range. Therefore, this indicates that the concentration of vacancy-type defects in the two films is consistent in the detectable depth range. The mean projective depth of energetic positron, R (nm), was estimated using the following equation [25],

$$R = \left(\frac{40}{\rho}\right)E^{1.6} \quad (1)$$

where E (keV) is the positron energy, ρ (g·cm^{-3}) is the density of materials, and 40 and 1.6 are the constant parameters that are related to a given W material. As we all know, the density of W materials is 19.35 g·cm^{-3}. Given this, the energy of 0.18–20.18 keV of the incident slow positrons corresponds to the mean projective range of 0.1∼253.1 nm according to the equation. This detection depth is deep enough to reflect the vacancy-type defect concentration of the whole film.

TDS spectra of W films and W-Ta-Cr-V films exposed to deuterium plasma to a fluence of 2.63 $\times$ 10^{24} D/m^2·s is shown in Fig. 8. A peculiar phenomenon of the bursting release of deuterium was found obviously in the range of 350 K-750 K, which is reflected in the appearance of many burrs on the TDS curve of W films (blue curve). The reason for this phenomenon is believed to be the instantaneous cracking of the W films during heating [26]. The bursting releases appeared in the range of 350 K to 750 K may be caused by the release of macroscopic stress during heating. It is well known that different positions of desorption peaks correspond to different deuterium trapping energies. In general, the desorption peak at low temperature range corresponds to the low trapping energy, while the desorption peak at high temperature range corresponds to the high trapping energy. In the TDS spectra of W films, several peaks appear in the range of 350 K to 1000 K. The first peak is located at around 373 K. Besides, two desorption peak locates at around 500 K and the additional one locates at around 600 K. A broad peak spanning 800 K to1000 K was found at the end of the spectrum. There is a peak near 850 K in this span. The TDS spectrum of W-Ta-Cr-V films (black curve) spectra in Fig. 8 shows that all deuterium release peaks are between 350 K and 800 K. The initial peak is located at around 373 K. Besides, the main desorption peak is located at around 500 K. The last peak is located at around 600 K.

Fig. 9 shows the total deuterium retention of the two films. The deuterium retention in the irradiated films was evaluated by integrating the deuterium release rate with respect to temperature. Deuterium retention in W-Ta-Cr-V films and W films is 27.01 $\times$ 10^{21} D/m^2 and 5.63 $\times$ 10^{21} D/m^2, respectively. Compared with W films, deuterium was captured by more grain boundary defects, resulting in deuterium retention by a factor of $\sim$ 5.

3.6. Nanoindentation

The nanoindentation test results are shown in Fig. 10. The hardness of the W-Ta-Cr-V films has been measured before and after irradiation, which is approximately 20.94 GPa and 22.51 GPa, respectively. The results show that the hardness of the two films increased significantly after irradiation, which is due to the presence of irradiation defect clusters such as dislocation loops and vacancy-type defects will increase the hardness of the material by acting as obstacles to the glide of dislocations. Besides, the hardness increase value ΔH of the W films before and after irradiation is 3.63 GPa, while the hardness increase value ΔH of the W-Ta-Cr-V films before and after irradiation is 1.57 GPa. The lower ΔH of W-Ta-Cr-V films may be attributed to the radiation-induced void defects in W-Ta-Cr-V films are less (details in the discussion section), so void hardening is not the main factor. This may be the reason why the increase in hardness of W-Ta-Cr-V films after irradiation is lower than that of pure W films.

4. Discussion

As mentioned above, the following four main phenomena can be obtained by comparing the measurement results of W films and W-Ta-Cr-V films before and after exposed to deuterium plasma. (a) High-temperature desorption peak within the range of 800–1000 K

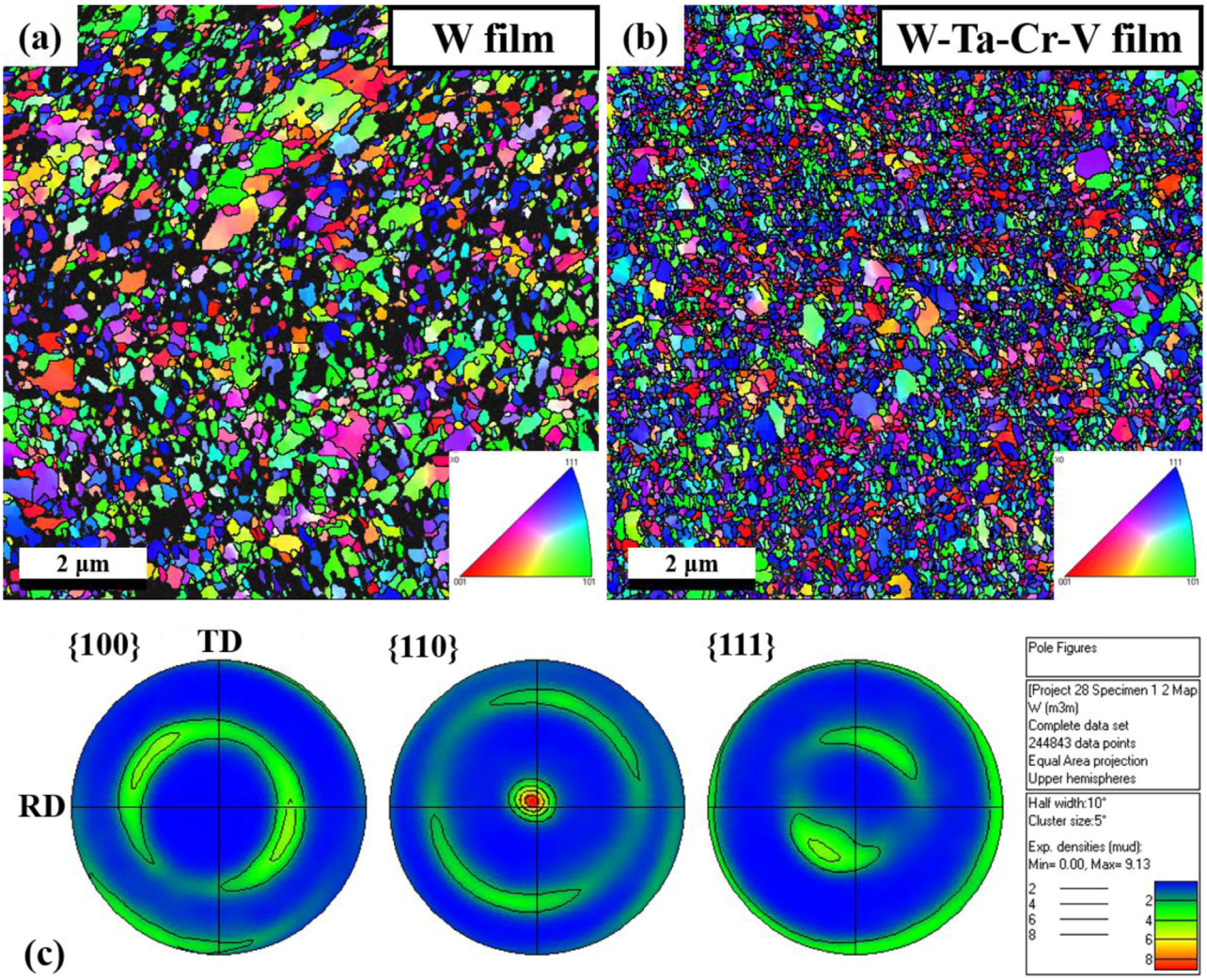

Fig. 5. Inverse pole figure (IPF) maps of the W film (a), W-Ta-Cr-V film (b) after annealing at 1000 °C, and pole figures {110} of W-Ta-Cr-V film (c).

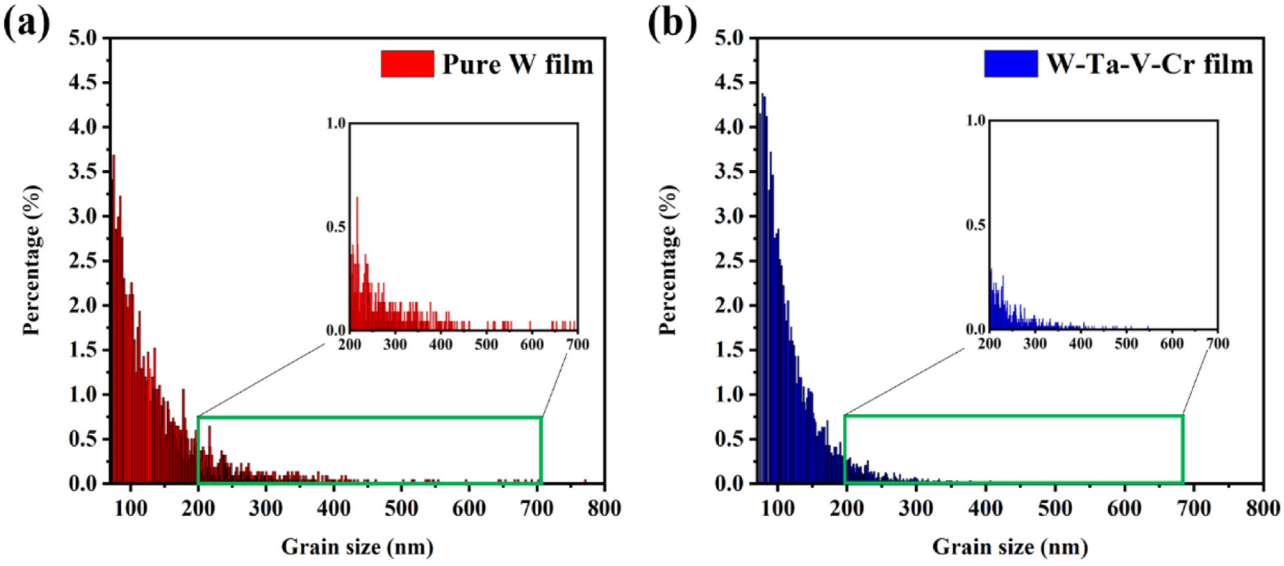

Fig. 6. Bar graphs of the grain size statistical distribution of W films (a) and W-Ta-Cr-V films (b) after annealing at 1000 °C.

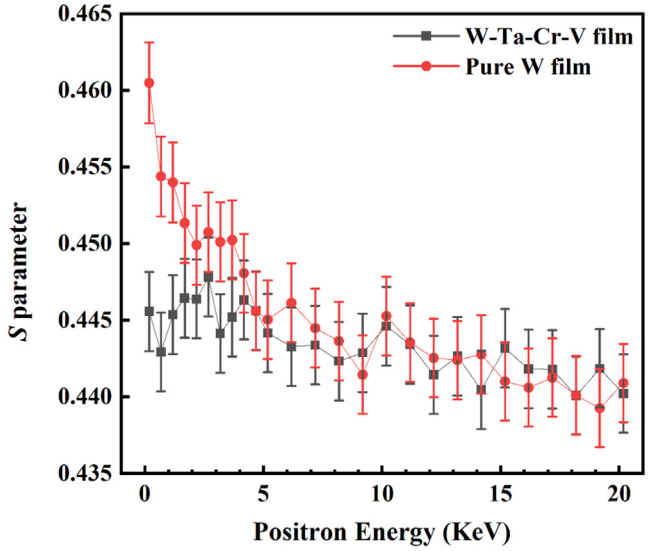

Fig. 7. *S* parameter versus depth for W film and W-Ta-Cr-V film without deuterium plasma irradiation.

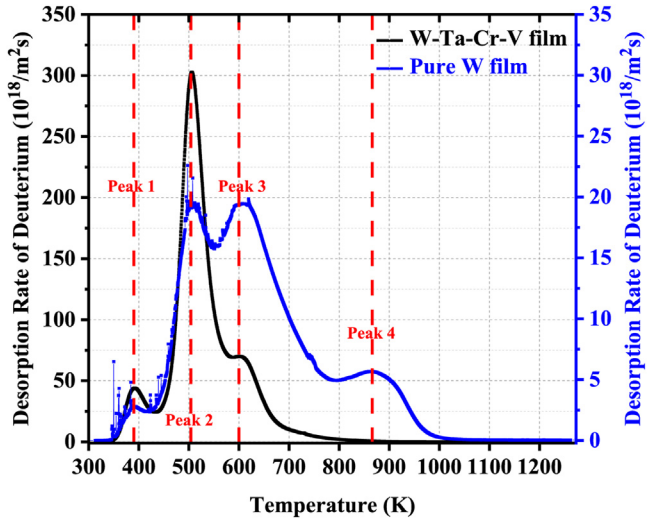

Fig. 8. TDS spectra of W film and W-Ta-Cr-V film irradiated by 110 eV deuterium plasma to a fluence of 2.63 × 10^{24} D/m^2.

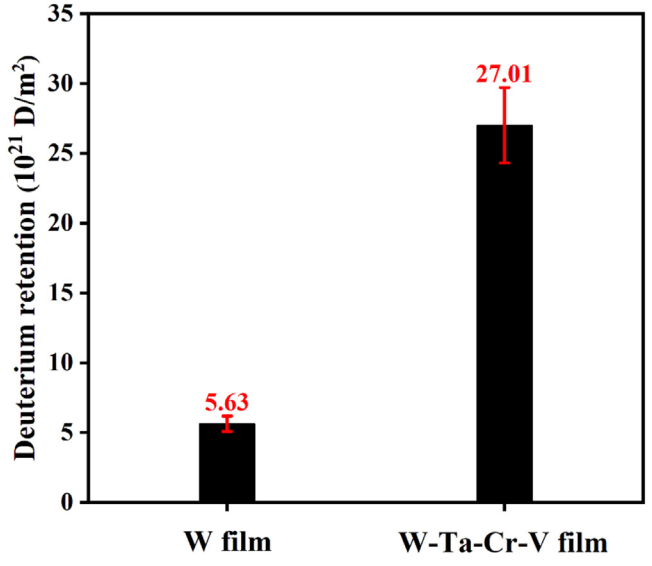

Fig. 9. Total deuterium retention in W film and W-Ta-Cr-V film.

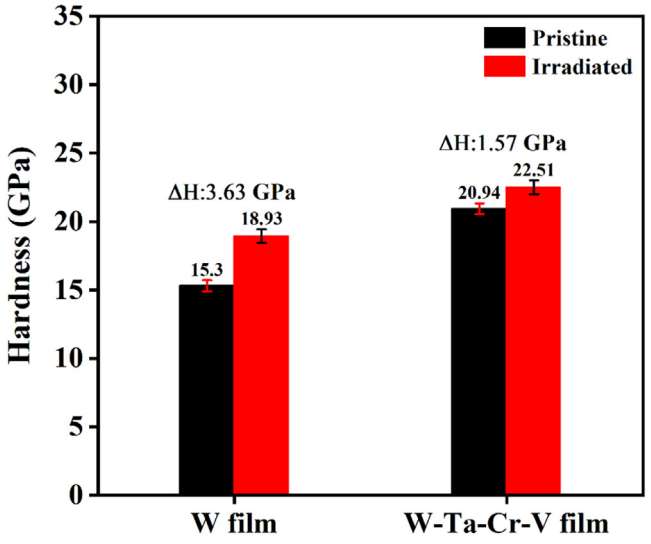

Fig. 10. Hardness of the films before and after the deuterium plasma irradiation.

disappeared in the W-Ta-Cr-V films measured by TDS; (b) The results of EBSD shows that the annealed W-Ta-Cr-V films have more grain boundary defects than W films; (c) The DBS-PA shows that the concentration of vacancy-defects in annealed W-Ta-Cr-V films is approximately the same as that in W films; (d) Difference of total retention between the two films irradiated by 110 eV deuterium plasma. The results show that the total deuterium retention in W-Ta-Cr-V films is more than 5 times higher than that of W films. The results will be discussed in turn below.

4.1. Desorption peaks in TDS spectra of W-Ta-Cr-V films

In general, the thermal desorption behaviors of deuterium are affected by the types of trap sites and their distribution. Deuterium retained in the sample is mainly trapped by various defects such as dislocations, grain boundaries, vacancies, vacancies clusters, and voids. Various types of defect trapping sites have different trapping energies [27]. The peaks in the span of 300 K to 800 K occur at roughly the same desorption temperature for W films and W-Ta-Cr-V films. The first peak locates at around 373 K and the second peak locates at around 500 K. The thermal desorption peak is located in the temperature range below 550 K, which can be attributed to the deuterium released from dislocations and grain boundaries [28]. It has been reported that the trapping energy of 0.85 eV, which can be attributed to deuterium retention by dislocations or grain boundaries [29,30]. Thus, it can be considered that the first and second thermal desorption peaks of W-Ta-Cr-V films are mainly due to the deuterium de-trapping from dislocations and grain boundaries, respectively. A higher deuterium trapping energy of the single vacancy and vacancy cluster in tungsten is 1.85 eV, the corresponding desorption peak temperature ranges roughly from 550 K to 800 K [29].

The third desorption peak of W films at around 600 K is related to the release of deuterium in vacancy defects [31,32]. Similarly, the last desorption peak at around 600 K in TDS spectra of W-Ta-Cr-V films corresponds to the deuterium de-trapped from vacancy defects. It is worth mentioning that the observed deuterium desorption in W-Ta-Cr-V films appears to be a narrower desorption temperature span (300 K∼800 K) causing all the deuterium to release from the sample. In the temperature range >800 K, there is no thermal desorption peak. However, the TDS spectra of the W films show a desorption peak in the temperature range of 800 K∼1000 K, which can be attributed to deuterium released from

vacancy-related defects with higher deuterium trapping energies. It should be noted that the low-energy deuterium is capable of creating a considerable number of vacancy-type defects in W, such a high-temperature desorption tail should be associated with the new vacancies created by the deuterium plasma [33,34]. This result has also been observed in previous investigations. The trapping energies corresponding to 2.1 eV (desorption temperature to 1000 K) are typically voids and the deuterium adsorbed on the inner surface of the voids [29].

4.2. Fewer and smaller vacancy-type defects inside the grains

4.2.1. Fewer vacancy-type defects inside the grains

The peak intensity of the second desorption peak in the spectra of W-Ta-Cr-V films is the highest. This makes sense since the finer grains in W-Ta-Cr-V films compared with W films and therefore contain more grain boundaries that presumably trap deuterium. As the grain boundaries may act as defect sinks for the implanted deuterium atoms, a large amount of deuterium is captured here.

It is well known that atoms on grain boundaries are disordered and there are many defects such as vacancies and dislocations. It makes sense that the concentration of vacancy defects at the grain boundary is higher than that inside the grain when the grain size is smaller. Obviously, the finer the original grain, the more grain boundaries. According to the results of EBSD, it can be concluded that the concentration of grain boundary defects of W-Ta-Cr-V films is higher than that of W films. In other words, the concentration of vacancy defects outside the grains in W-Ta-Cr-V films is greater than that of the W films. However, the results of DBS-PA show that the concentration of vacancy-type defects in W-Ta-Cr-V films is almost the same as the W films. As mentioned above, S parameter is sensitive to open volume defects because trapped state annihilation occurs at the vacancy-type defects. Therefore, the S parameter also reflects the concentration information of vacancy defects at the grain boundaries. As a result, the S parameters of the two films are almost equal. Combined with the results of DBS-PA and EBSD, it can be concluded that the concentration of vacancy defects inside the grain of W-Ta-Cr-V films is lower than that of W films. That is to say there are fewer vacancy-type defects in the grains of W-Ta-Cr-V films than that of W films.

4.2.2. Smaller vacancy-type defects inside the grains

No deuterium desorption in W-Ta-Cr-V films corresponding to the temperature range 800 K∼1000 K shown in TDS spectra. This indicates that there are no or few voids generated in W-Ta-Cr-V films induced by low-energy deuterium plasma irradiation, which may be due to the inhibition of the nucleation and growth of voids. It can be inferred that the composition complexity and large lattice distortion of W-Ta-Cr-V high entropy alloy leads to a stronger obstacle to the migration of vacancies, resulting in the inhibition of the nucleation and growth of voids. In the present study, δ (atomic size polydispersity) is defined by formula as follows [35]:

$$\delta = 100 \times \left[\sum_{i=1}^{n} C_i(1 - r_i/\bar{r})^2\right]^{1/2} \quad (2)$$

Where C_i and r_i are the atomic percentage and atomic radius of the ith element, $\bar{r}=\sum_{i=1}^{n} C_i r_i$ is the average atomic radius. The δ value of W-Ta-Cr-V films is ≈4.935, as shown in Table 1. The atomic size difference δ can evaluate the lattice distortion of high entropy alloys.

According to the common form of the void growth equation [36]:

$$\frac{dR}{dt} = \dot{R} = \frac{\Omega}{R}\left[D_v\left(C_v - C_v^V\right) - D_i C_i\right] \quad (3)$$

Where R is the radius of void, Ω is the defect volume, $C_{i,v}$ is vacancy/interstitial concentration in the solid, C_v^V is vacancy concentration at the void surface, and thermal emission of interstitials from voids is neglected. C_v^V is the vacancy concentration at the void surface, which is expressed as:

$$C_v^V = \frac{1}{\Omega} exp\left(\frac{S_v^f}{k}\right) exp\left(-\frac{E_v^f}{kT}\right) exp\left(-\frac{p\Omega}{kT}\right) = C_v^0 exp\left(\frac{2\gamma\Omega}{RkT}\right) \quad (4)$$

Where S_v^f is the vacancy formation entropy, k is the Boltzmann constant, T is the absolute temperature, and p is the surface tension of a void ($p = -\frac{2\gamma}{R}$, γ is the surface energy). C_v^0 is the thermal equilibrium concentration of vacancies in a solid material:

$$C_v^0 = \frac{1}{\Omega} exp\left(\frac{S_v^f}{k}\right) exp\left(-\frac{E_v^f}{kT}\right) \quad (5)$$

Here, it is reasonable to imagine that the formation of a monovacancy in a high-entropy alloy would correspond to a higher change in entropy due to more kinds of atomic arrangements than in pure metal W. Thus, the vacancy formation entropy S_v^f of HEA film is higher than that of W film according to the definition of entropy. The vacancy formation energy E_v^f is approximately proportional to the melting point (T_m) of the solid material. The T_m of W-Ta-Cr-V films is obviously lower than the value of W, which can be attributed to the three transition metal elements Ta, Cr and V, has a much lower T_m than W films, (as shown in Table 1). Thus, W-Ta-Cr-V films possess lower E_v^f compared with W film and a larger equilibrium thermal vacancy concentration C_v^0. Assuming other variables are nearly identical, it can deduce that a larger value of C_v^0 results in a larger value of C_v^V, and we then obtain a smaller $\frac{dR}{dt}$ value. The lower E_v^f therefore greatly slows down the nucleation and growth of void. To sum up, the growth of cavities induced by low-energy deuterium plasma irradiation in W-Ta-Cr-V films was inhibited.

4.3. Higher deuterium retention

Deuterium retention in solid material could be absorbed in two ways: trapping by the defects and chemical absorption by elements. Deuterium reacts with many different elements to form various compounds. Most of Group III–V non-metallic elements, as well as light simple metals of Group I–IV, form covalently bonded molecules or crystals, whereas most heavy simple metals do not form any compounds with deuterium [38]. The transition metal elements Ta, Cr, and V do not form any compounds with deuterium [39,40]. Therefore, only deuterium trapped by defects in the material contributes to the total retention. It is obvious that the deuterium retention of W-Ta-Cr-V film is higher than that of W film. As shown in Fig. 11, Gaussian peak fitting was performed on the thermal desorption spectra of the two samples to quantitatively analyze the desorption of deuterium in different defect types. It should be noted that there is a deviation between the total retention after fitting and the total deuterium retention of the actual thermal desorption spectrum.

Table 2 shows the Gaussian peak fitting results of thermal desorption spectra of W film and W-Ta-Cr-V film, and the percentage of deuterium desorption after fitting. It is found that the deuterium retention in the W-Ta-Cr-V films is mainly captured by the grain boundary defects, and the proportion of deuterium desorption in the grain boundary is ∼66.43% (Peak Fit 2 of W-Ta-Cr-V films). The more important finding is that the desorption of deuterium from the grain boundary in the W-Ta-Cr-V film is ∼31.7 times than that of the W film. This can be interpreted as the result of EBSD indicating that W-Ta-Cr-V film has more grain boundary defects. In addition, the deuterium desorption from vacancy-type defects is ∼1.2 times that of the W film, indicating that the concentration of

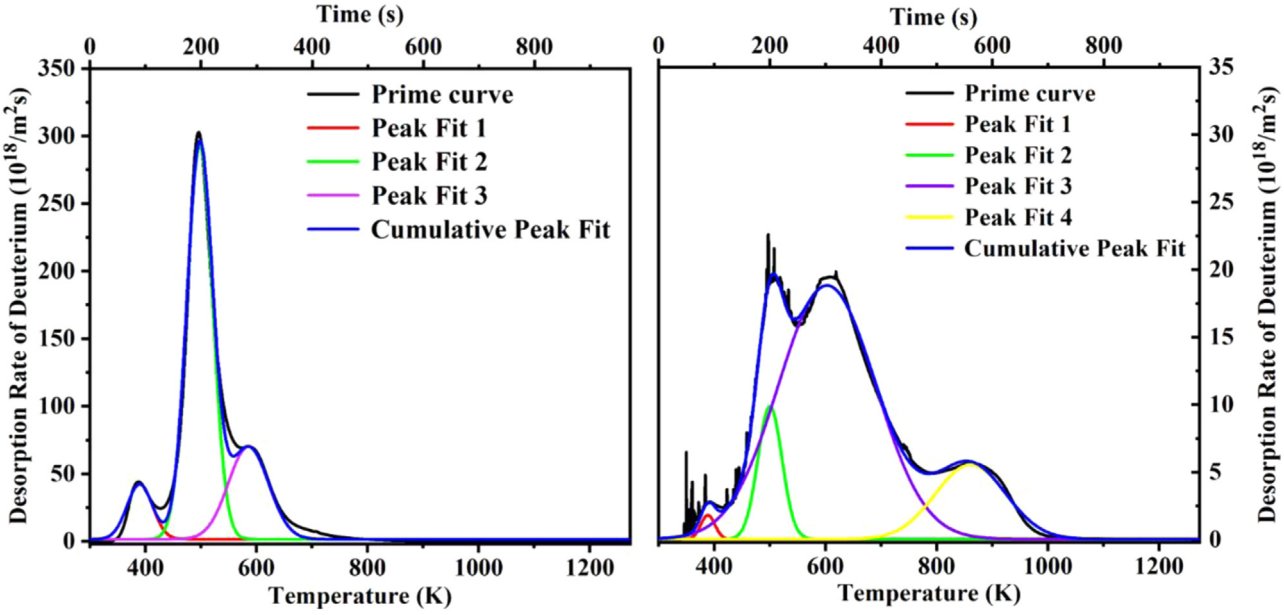

Fig. 11. (a) and (b) are the Gaussian fitting peaks of deuterium trapped by different defect types in W-Ta-Cr-V film and W film.

Table 2
Gaussian peak fitting results of thermal desorption spectra.

Gaussian peak fitting of thermal desorption spectra of W film and W-Ta-Cr-V film, and the percentage of deuterium desorption in the Gaussian peak fitting.	W film	W-Ta-Cr-V film
	Deuterium desorption (10^{20} D/m^2)	
Peak fit 1	0.56 (± 0.02)	23.44 (± 0.34)
Percentage (%)	1.00% (± 0.03%)	9.19% (±0.13%)
Peak fit 2	5.34 (± 0.06)	169.39 (± 0.55)
Percentage (%)	9.57% (± 0.1%)	66.43% (±0.21%)
Peak fit 3	41.20 (± 0.12)	62.15 (± 0.65)
Percentage (%)	73.75% (± 0.3%)	24.38% (±0.25%)
Peak fit 4	8.76 (± 0.06)	/
Percentage (%)	15.69% (± 0.1%)	/
Cumulative Peak Fit	55.86 (± 0.26)	254.98 (± 1.54)
Percentage (%)	100.00%	100.00%

vacancy-type defects in W-Ta-Cr-V film is approximately the same as that in the W film. This is consistent with the result of DBS-PA. Therefore, the W-Ta-Cr-V film has more grain boundary defects than the W film, which is the reason for its higher deuterium retention.

5. Conclusion

In summary, a novel of tungsten-containing high-entropy alloy films based on four elements: W, Ta, Cr and V, is prepared by magnetron sputtering. The microstructure of the films was checked by XRD and confirmed to be *bcc* single-phase structure before irradiation. In this work, the deuterium retention and desorption behavior of W-Ta-Cr-V films under 110 eV deuterium plasma irradiation with a fluence of 2.63×10^{24} D/m^2, and the pure W film were used as the reference sample. The EBSD results show that the average grain size of W-Ta-Cr-V films is smaller than that of the pure W films, indicating that there are more grain boundary defects in W-Ta-Cr-V films than W films. However, the DBS-PA results show that the concentration of vacancy-type defects in the two films is almost the same. Combining the results of TDS, it can be concluded that there are fewer vacancy-type defects inside the grains of the W-Ta-Cr-V films, and the nucleation and growth of void defects are inhibited. Compared with the W film, the deuterium retention in W-Ta-Cr-V film is nearly 5 times higher. More deuterium captured by grain boundary defects increases deuterium retention in W-Ta-Cr-V films. Due to the high deuterium retention of W-Ta-Cr-V films, it should be carefully considered in the design of high entropy alloys for applications in fusion reactors.

Declaration of Competing Interest

The authors declare that they have no known competing financial interests or personal relationships that could have appeared to influence the work reported in this paper.

Acknowledgments

The authors are grateful for the financial support by National Natural Science Foundation of China with Grant No. 11675010, and National Magnetic Confinement Fusion Energy Research Project with Grant No. 2019YFE03120003.

CRediT authorship contribution statement

Kaigui Zhu: Conceptualization, Writing - Review & Editing, Supervision, Funding acquisition. **Yongzhi Shi:** Investigation, Data Curation, Writing - original draft, Visualization. **Zhenyu Jiang:** Investigation. **Tongjun Xia:** Investigation. **Zizhao Wang:** Investigation. **Jianwei Wu:** Investigation. **Xingzhong Cao:** Investigation.

References

[1] P.K. Huang, J.W. Yeh, T.T. Shun, S.K. Chen, Multi-Principal-Element Alloys with Improved Oxidation and Wear Resistance for Thermal Spray Coating, Adv. Eng. Mater. 6 (2004) 74–78.

[2] J.W. Yeh, S.K. Chen, S.j. Lin, J.Y. Gan, T.S. Chin, T.T. Shun, C.H. Tsau , Nanostructured High-Entropy Alloys with Multiple Principal Elements: Novel Alloy Design Concepts and Outcomes, Adv. Eng. Mater. 5 (2004) 299–303.

[3] Y. Zhang, Y.J. Zhou, J.P. Lin, G.L. Chen, P.K. Liaw, Solid-Solution Phase Formation Rules for Multi-component Alloys, Adv. Eng. Mater. 10 (2008) 534–538.

[4] J.W. Yeh, Alloy Design Strategies and Future Trends in High-Entropy Alloys, JOM-J. Miner. Met. Mater. Soc. 65 (2013) 1759–1771.

[5] T. Shi, P.H. Lei, X. Yan, J. Li, Y. Di Zhou, Y.P. Wang, Z.X. Su, Y.K. Dou, X.F. He, Di Yun, W. Yang, C.Y. Lu, Current development of body-centered cubic high-entropy alloys for nuclear applications, Tungsten 385 (2021) 217.

[6] T. Egami, M. Ojha, O. Khorgolkhuu, D.M. Nicholson, G.M. Stocks , Local Electronic Effects and Irradiation Resistance in High-Entropy Alloys, JOM-J. Miner. Met. Mater. Soc. 67 (2015) 2345–2349.

[7] T.D. Shen, Radiation tolerance in a nanostructure:Is smaller better? Nucl. Instrum. Methods Phys. Res. Sect. B 266 (2008) 921–925.

[8] P.M. Piaggi, E.M. Bringa, R.C. Pasianot, N. Gordillo, M. Panizo-Laiz, J. del Río, C. Gómez de Castro, R. Gonzalez-Arrabal, Hydrogen diffusion and trapping in nanocrystalline tungsten, J. Nucl. Mater. 458 (2015) 233–239.

[9] Y. Zhang, K. Jin, H. Xue, C. Lu, R.J. Olsen, L.K. Beland, M.W. Ullah, S. Zhao, H. Bei, D.S. Aidhy, G.D. Samolyuk, L. Wang, M. Caro, A. Caro, G.M. Stocks, B.C. Larson, I.M. Robertson, A.A. Correa, W.J. Weber, Influence of chemical disorder on energy dissipation and defect evolution in advanced alloys, J. Mater. Res. 31 (2016) 2363–2375.

[10] S. Zhao, G.M. Stocks, Y. Zhang, Defect energetics of concentrated solid-solution alloys from ab initio calculations, Phys. Chem. Chem. Phys. 18 (2016) 24043–24056.

[11] S. Zhao, T. Egami, G.M. Stocks, Y. Zhang, Effect of d electrons on defect properties in equiatomic NiCoCr and NiCoFeCr concentrated solid solution alloys, Phys. Rev. Materials 2 (2018) 1–8.

[12] C. Lu, L. Niu, N. Chen, K. Jin, T. Yang, P. Xiu, Y. Zhang, F. Gao, H. Bei, S. Shi, M.-.R. He, I.M. Robertson, W.J. Weber, L. Wang, Enhancing radiation tolerance by controlling defect mobility and migration pathways in multicomponent single-phase alloys, Nat. Commun. 7 (2016) 1–8.

[13] S. Xia, X. Yang, T. Yang, et al., Irradiation Resistance in AlxCoCrFeNi High Entropy Alloys, JOM-J. Miner. Met. Mater. Soc. 67 (2015) 2340–2344.

[14] L. Yang, H. Ge, et al., High He-ion irradiation resistance of CrMnFeCoNi high-entropy alloy revealed by comparison study with Ni and 304SS, J. Mater. Sci. Technol. 35 (2019) 74–79.

[15] O. El-Atwani, N. Li, M. Li, A. Devaraj, J.K.S. Baldwin, M.M. Schneider, D. Sobieraj, Outstanding radiation resistance of tungsten-based high-entropy alloys, Sci. Adv. 5 (2019) 1–9.

[16] S. Zhao, Defect properties in a VTaCrW equiatomic high entropy alloy (HEA) with the body centered cubic (bcc) structure, J. Mater. Sci. Technol. 44 (2020) 133–139.

[17] J. Yu, W. Han, Z. Chen, K. Zhu, Comparison of blistering of W bulk and film deposited by magnetron sputtering under helium irradiation, Nucl. Mater. Energy 12 (2017) 588–592.

[18] T. Xia, Z. Wang, Z. Jiang, Y. Shi, J. Wu, X. Ren, K. Zhu, Evolution of surface morphology and helium bubble in tungsten under 40 keV helium ions implantation followed by deuterium plasma exposure, Phys. Scr. 97 (2022) 55602.

[19] C. Li, X. Cao, X. Ning, F. Liu, B. Wang, P. Zhang, L. Wei, D. Li, Implantation profiles and depth distribution of slow positron beam simulated by Geant4 toolkit, Phys. Scr. 94 (2019) 1–8.

[20] A. Debelle, M.F. Barthe, T. Sauvage, First temperature stage evolution of irradiation-induced defects in tungsten studied by positron annihilation spectroscopy, J. Nucl. Mater. 376 (2008) 216–221.

[21] J. Yan, X. Li, Z. Wang, K. Zhu, Comparison of surface morphologies and helium retention of nanocrystalline W and W-Cr films prepared by magnetron sputtering, Nucl. Mater. Energy 22 (2020) 1–5.

[22] L.R. Owen, N.G. Jones, Lattice distortions in high-entropy alloys, J. Mater. Res. 33 (2018) 2954–2969.

[23] J.W. Yeh, S.Y. Chang, Y.D. Hong, S.K. Chen, S.J. Lin, Anomalous decrease in X-ray diffraction intensities of Cu–Ni–Al–Co–Cr–Fe–Si alloy systems with multi-principal elements, Mater. Chem. Phys. 103 (2007) 41–46.

[24] Z. Chen, L. Niu, Z. Wang, L. Tian, L. Kecskes, K. Zhu, Q. Wei, A comparative study on the in situ helium irradiation behavior of tungsten, Acta Mater. 147 (2018) 100–112.

[25] K. Saarinen, P. Hautojarvi, A. Vehanen, R. Krause, G. Dlubek, Shallow positron traps in GaAs, Phys. Rev. B-Condens Matter 39 (1989) 5287.

[26] W.M. Shu, M. Nakamichi, V.K. Alimov, G.N. Luo, K. Isobe, T. Yamanishi, Deuterium retention, blistering and local melting at tungsten exposed to high-fluence deuterium plasma, J. Nucl. Mater. (2009) 1017–1021 390-391.

[27] R. Zhang, H. Zhou, J. Yu, W. Han, M. Liu, C. Chen, K. Zhu, Effect of vanadium alloying on irradiation performance of tungsten under 60 keV helium irradiation, J. Nucl. Mater. 512 (2018) 65–71.

[28] A. Rusinov, Y. Gasparyan, N. Trifonov, A. Pisarev, S. Lindig, M. Sakamoto, Investigation of hydrogen-defect interaction in tungsten by the probe fluence method, J. Nucl. Mater. 415 (2011) S645–S648.

[29] O.V. Ogorodnikova, B. Tyburska, V.K. Alimov, K. Ertl, The influence of radiation damage on the plasma-induced deuterium retention in self-implanted tungsten, J. Nucl. Mater. 415 (2011) S661–S666.

[30] W. Han, K. Zhu, J. Yan, T. Xia, Z. Wang, X. Ye, C.A. Chen, J. Wu, Y. Ma, Blistering and deuterium retention in Nb-doped W exposed to low-energy deuterium plasma, Nucl. Mater. Energy 23 (2020) 100741.

[31] H. Zhang, X. Zhang, L. Qiao, P. Wang, Comparing deuterium retention in heavy ion damaged tungsten measured by glow discharge optical emission spectroscopy, nuclear reaction analysis and thermal desorption spectroscopy, Phys. Scr. 96 (2021) 115602.

[32] H. Zhou, S. Wang, R. Zhang, C. Chen, K. Zhu, Effect of pre-damage induced by argon ions on the following 60 keV helium ions irradiation behavior of tungsten-tantalum alloy, Fusion Eng. Des. 154 (2020) 111533.

[33] X.L. Zhu, Y. Zhang, L. Cheng, Y. Yuan, G. de Temmerman, B.Y. Wang, X.Z. Cao, G.H. Lu, Deuterium occupation of vacancy-type defects in argon-damaged tungsten exposed to high flux and low energy deuterium plasma, Nucl. Fusion 56 (2016) 36010.

[34] R. Zhang, H. Zhou, J. Yu, W. Han, M. Liu, C. Chen, K. Zhu, Effect of vanadium alloying on irradiation performance of tungsten under 60 keV helium irradiation, J. Nucl. Mater. 512 (2018) 65–71.

[35] D.J.M. King, S.C. Middleburgh, A.G. McGregor, M.B. Cortie, Predicting the formation and stability of single phase high-entropy alloys, Acta Mater. 104 (2016) 172–179.

[36] G.S. Was, **Fundamentals of radiation materials science: metals and alloys [M]**, springer (2016).

[37] S. Guo, C.T. Liu, Phase stability in high entropy alloys, Prog. Nat. Sci. 21 (2011) 433–446.

[38] Y. Fukai, The Metal-Hydrogen System [M], Mater. Sci. 21 (2005) 1–499.

[39] K.Takase S.Ohnuki, K. Yashiki, K. Hamada, T. Suda, S. Watanabe, In-situ Observation of Hydride Stability of Vanadium Alloys in Electron Microscope, Korean J. Microscopy 36 (2) (2006) 57–61.

[40] Y. Zayachuk, M.H.J.'t. Hoen, P.A. van Zeijlmans Emmichoven, D. Terentyev, I. Uytdenhouwen, G. van Oost, Surface modification of tungsten and tungsten—tantalum alloys exposed to high-flux deuterium plasma and its impact on deuterium retention, Nucl. Fusion 53 (2013) 13013.